Am J Physiol Endocrinol Metab 311: E380–E395, 2016.
First published June 21, 2016; doi:10.1152/ajpendo.00104.2016.

Proposed mechanisms for oligonucleotide IMT504 induced diabetes reversion in a mouse model of immunodependent diabetes

María S. Bianchi,[1] Stefanía Bianchi,[1] Andrés Hernado-Insúa,[2] Leandro M. Martinez,[1] Néstor Lago,[3] Carlos Libertun,[1,3] Norma A. Chasseing,[1] Alejandro D. Montaner,[2] and Victoria A. Lux-Lantos[1]

[1]*Instituto de Biología y Medicina Experimental (IBYME-CONICET), Buenos Aires, Argentina;* [2]*Fundación Pablo Cassará (ICT Milstein-CONICET), Buenos Aires, Argentina; and* [3]*Facultad de Medicina, Universidad de Buenos Aires. Buenos Aires, Argentina*

Submitted 17 March 2016; accepted in final form 7 June 2016

Bianchi MS, Bianchi S, Hernado-Insúa A, Martinez LM, Lago N, Libertun C, Chasseing NA, Montaner AD, Lux-Lantos VA. Proposed mechanisms for oligonucleotide IMT504 induced diabetes reversion in a mouse model of immunodependent diabetes. *Am J Physiol Endocrinol Metab* 311: E380–E395, 2016. First published June 21, 2016; doi:10.1152/ajpendo.00104.2016.—Type 1 diabetes (T1D) originates from autoimmune β-cell destruction. IMT504 is an immunomodulatory oligonucleotide that increases mesenchymal stem cell cloning capacity and reverts toxic diabetes in rats. Here, we evaluated long-term (20 doses) and short-term (2–6 doses) effects of IMT504 (20 $mg \cdot kg^{-1} \cdot day^{-1}$ sc) in an immunodependent diabetes model: multiple low-dose streptozotocin-injected BALB/c mice (40 $mg \cdot kg^{-1} \cdot day^{-1}$ ip for 5 consecutive days). We determined blood glucose, glucose tolerance, serum insulin, islet morphology, islet infiltration, serum cytokines, progenitor cell markers, immunomodulatory proteins, proliferation, apoptosis, and islet gene expression. IMT504 reduced glycemia, induced β-cell recovery, and impaired islet infiltration. IMT504 induced early blood glucose decrease and infiltration inhibition, increased β-cell proliferation and decreased apoptosis, increased islet indoleamine 2,3-dioxygenase (IDO) expression, and increased serum tumor necrosis factor and interleukin-6 (IL-6). IMT504 affected islet gene expression; *preproinsulin-2*, *proglucagon*, *somatostatin*, *nestin*, *regenerating gene-1*, and *C-X-C motif ligand-1 cytokine* (*Cxcl1*) increased in islets from diabetic mice and were decreased by IMT504. IMT504 downregulated *platelet endothelial cell adhesion molecule-1* (*Pecam1*) in islets from control and diabetic mice, whereas it increased *regenerating gene-2* (*Reg2*) in islets of diabetic mice. The IMT504-induced increase in IL-6 and islet IDO expression and decreased islet *Pecam1* and *Cxcl1* mRNA expression could participate in keeping leukocyte infiltration at bay, whereas upregulation of *Reg2* may mediate β-cell regeneration. We conclude that IMT504 effectively reversed immunodependent diabetes in mice. Corroboration of these effects in a model of autoimmune diabetes more similar to human T1D could provide promising results for the treatment of this disease.

β-cells; insulitis; serum cytokines; islet gene expression

TYPE 1 DIABETES (T1D) is a progressive autoimmune destruction of β-cells. To prevent or cure T1D, research has aimed largely at understanding and modulating immunological responses (19, 43) and/or restoring β-cell mass, which is limited by the availability of transplantable β-cells and the need for chronic immunosuppression (1). Furthermore, mesenchymal stem cells (MSCs) have been assayed as cell-based treatments for inflammatory disorders, including T1D (27), since they promote immunomodulation and regeneration (47). However, their translation into clinic has remained problematic (26). An exciting alternative to MSC transplantation, but one related to it, consists in using therapeutic agents that can stimulate endogenous MSC expansion in the affected being.

Immunomodulatory oligonucleotides (ODNs) are synthetic molecules that activate immune cells. Two classes of ODNs have been identified, CpG ODNs (29) and non-CpG ODNs. Our group has identified a class of non-CpG ODNs called PyNTTTTGT, characterized for their active site (Py is C or T, and N is A, T, C, or G). IMT504, the prototype of this class, has two specific PyNTTTTGT sequences in its molecule (41). CpG and PyNTTTTGT ODNs have a number of common characteristics but also remarkable differences (41). Among the latter: *1*) PyNTTTTGT ODNs do not induce IFNα secretion (13), *2*) they stimulate granulocyte-macrophage colony-stimulating factor (GM-CSF) secretion in human CD56+ (NK/NKT) cells (42), and *3*) they stimulate in vivo and in vitro MSCs proliferation (22). Interestingly, IMT504 stimulated CD56+ NKT cells that have been postulated to convey peripheral tolerance and protection against autoimmune diabetes (30). IMT504 also promoted marked improvement in rat models of bone injury (22), neuropathic pain (7), and sepsis (5). Regarding diabetes, streptozotocin-induced toxic diabetes in rats was reversed by IMT504, improving glycemia, increasing islet number, β-cell content, β-cell proliferation, and early expression of pancreatic progenitor markers (3). Although IMT504 is active in rat and human cells, we have not yet demonstrated its effects in mice.

Since IMT504 has both immunomodulatory and regenerative properties, we investigated its actions in multiple low-dose streptozotocin-treated mice here, a model of immunodependent diabetes (48) that shares certain characteristics with human T1D.

MATERIALS AND METHODS

Oligonucleotides

HPLC purified ODNs with phosphorothioate internucleotide linkages were purchased from Oligos Etc. ODNs were suspended in depyrogenated water, assayed for lipopolysaccharide contamination, and kept at −20°C until they were used. Quality was verified as described (22).

IMT504 is a 24-mer ODN (5′-TCATCATTTTGTCATTTTGTCATT-3′). For the in vivo experiments, a control ODN consisting of 24-mer poly C ODN was used. For the in vitro experiments, CpG ODN 1826 (5′-TCCATGACGTTCCTGACGTT-3′), a specific mouse TLR9 agonist, was also tested.

Address for reprint requests and other correspondence: V. Lux-Lantos, Vuelta de Obligado 2490 (C1428ADN), Buenos Aires, Argentina (e-mail: vlux@ibyme.conicet.gov.ar).

Animals

Male 6- to 8-wk-old BALB/c mice from the IBYME colony were housed in groups in a temperature-controlled room, with lights on from 0700 to 1900 and free access to laboratory chow and tap water.

Experimental procedures were performed according to protocols approved by the Institutional Animal Care and Use Committee at Instituto de Biología y Medicina Experimental in accordance with the Division of Animal Welfare, Office for Protection from Research Risks, National Institutes of Health, Animal Welfare Assurance for the Institute of Biology and Experimental Medicine A#5072-01. All possible steps were taken to avoid animal suffering at each stage of the experiments.

Experimental Immunodependent Diabetes

Immunodependent diabetes was induced in mice by intraperitoneal (ip) injection of multiple low (subdiabetogenic) doses of streptozotocin (MLDS). Streptozotocin (STZ; Sigma-Aldrich, St. Louis, MO) was freshly diluted in 0.05 M sodium citrate buffer (pH 4.5), 40 mg/kg body wt, and injected daily for 5 consecutive days at noon. In this model, diabetes develops only when STZ induces both β-cell toxicity and T cell-dependent immune reactions (48). Control animals were injected with citrate buffer. It took 15–20 days to observe consistent hyperglycemia. Only STZ-treated animals showing nonfasted blood glucose of ≥12 mM were considered diabetic. Glycemia in nonfasted control mice was 7.6 ± 0.2 mM.

Preliminary Studies

Dose-response study. A dose-response effect of IMT504 on blood glucose in immunodependent diabetic mice was performed to determine the optimal dose in this species. MLDS mice (blood glucose ≥12 mM) and control mice were treated with IMT504 doses of 2, 10, or 20 mg·kg body $wt^{-1}\cdot day^{-1}$. Animals were randomly assigned to the treatment groups and injected subcutaneously (sc) for 10 consecutive days (*days 1–10*). The groups were as follows: control-IMT504 (2), control-IMT504 (10), control-IMT504 (20), STZ-IMT504 (2), STZ-IMT504 (10), and STZ-IMT504 (20). Control diabetic and nondiabetic animals received saline (STZ-Saline, control-saline). Nonfasted glycemia was determined on *day 1* before treatment initiation and on *day 11* (1 day after the last IMT504 injection). Percentages of animals responding to treatment were calculated (n = 5–7).

In vitro bone marrow fibroblast colony-forming units. To assess whether IMT504 was able to stimulate the cloning efficiency of MSCs [fibroblast colony-forming unit (CFU-F) assay], mice were anesthetized with ketamine-xylazine (50/5 mg/kg) and euthanized for bone marrow (BM) harvesting. Procedures were performed as described previously (22). Briefly, after epiphyses were removed and access to the marrow cavities was gained, whole BM plugs were flushed out from femoral bones using a 1-ml syringe with α-medium (α-MEM; Gibco) supplemented with 100 IU/ml gentamicin, 25 IU/ml heparin (Larjan, Buenos Aires, Argentina), and 2.5 μg/ml amphotericin B (PAA Laboratories, Pasching, Austria). The cell suspension was centrifuged at 400 *g* for 10 min, and the pellet was suspended in fresh medium. This procedure was repeated twice. Cell concentration was evaluated by microscopic cell counting using a Neubauer hemocytometer in samples treated with 3% acetic acid. Cell viability was determined using the trypan blue staining method.

The cloning efficiency of BM-MSC was evaluated by CFU-F assay (1 MSC = 1 CFU-F). BM cells (3×10^6/well) were seeded in 25-cm^2 tissue culture flasks (Orange Scientific) containing α-medium supplemented with 100 IU/ml gentamicin (Gibco), 2.5 μg/ml amphotericin B (Gibco), 2 mM L-glutamine (Sigma-Aldrich), and 10% FCS (Gibco) and incubated at 37°C under a 5% CO_2 atmosphere, as described previously. Cultures were treated with a single dose of 4 μg/ml IMT504, 4 μg/ml CpG ODN 1826, or PBS (control) and incubated for 7 days. After a 7-day culture, nonadherent cells were removed by washing twice with PBS. Thereafter, fresh medium was added, and incubation proceeded for 7 more days under the same conditions. On *day 14*, cells were washed twice with PBS, fixed with 100% methanol for 15 min, and stained using Giemsa solution (Merck). Cells and colonies were observed and counted using an optical microscope. A CFU-F was defined as a group of at least 50 cells with an approximately circular disposition. The number of colonies counted in each culture treated with PBS (controls) was considered 100%. The percent variation with regard to controls in each experiment was calculated for each stimulus (n = 12).

First Experimental Design: Long-Term Effects of IMT504 in Diabetic Mice

MLDS mice (blood glucose ≥12 mM) and control mice were injected sc with IMT504 (20mg/kg BW) or saline, respectively, for 10 consecutive days (*days 1–10*) and then for 5 consecutive days starting on *days 21* and *36* (total no. of doses: 20). Glycemia was measured in tail blood samples in nonfasted conditions on *days 1*, *6*, *11*, *17*, *21*, *26*, *29*, *32*, *36*, *41*, *46*, *53*, and *66* at 11–12 AM (last IMT504 injection on *day 40*). Intraperitoneal glucose tolerance tests (IPGTT) were performed on *day 60*. On *day 67*, mice were anesthetized with 2% wt/vol avertin (12 ml/kg ip; Sigma-Aldrich), an intracardiac blood sample was obtained for serum cytokine determinations, and mice were then euthanized by transcardiac perfusion with 0.9% saline followed by 4% paraformaldehyde in PBS, pH 7.4. Pancreases were excised and processed for immunohistochemistry (n = 6–8) (3).

Blood Glucose

Blood glucose was monitored in tail blood samples using a One touch Ultra glucose meter (LifeScan, New Brunswick, NJ); strips were kindly donated by Johnson & Johnson.

IPGTT

IPGTTs were performed on *day 60* in mice from the first experimental design. Overnight-fasted animals were injected ip with 2 g/kg BW glucose, and glycemia was evaluated at 0, 30, 60, 90, and 120 min post-glucose administration (3).

Serum Insulin

Insulin was determined using an ultrasensitive mouse insulin ELISA kit (Crystal Chem, Chicago, IL) in serum samples obtained from tail blood at *time 0* during the IPGTT on *day 60*, as described (3).

HOMA-IR and HOMA-β-Cell

HOMA-IR and HOMA-β-cell indexes were calculated using the overnight-fasted blood glucose and serum insulin levels in the first experimental design and the 3-h-fasted blood glucose and serum insulin levels in the second experimental design:

$$\text{HOMA-IR} = \text{fasting insulin}\,(\mu\text{U/ml}) \times \text{fasting glucose}\,(\text{mmol/l})/22.5$$

$$\text{HOMA-}\beta\text{-cell} = 20 \times \text{fasting insulin}\,(\mu\text{U/ml})/\left[\text{fasting glucose}\,(\text{mmol/l}) - 3.5\right].$$

Leukocyte Infiltration

Five-micrometer pancreas sections from all animals (n = 4–6) were stained with hematoxylin-eosin and analyzed by light microscopy. Insulitis scoring was evaluated according to the following criteria: no insulitis (score 0); peri-insulitis, insulitis restricted to the periphery of islets (score 1); moderate insulitis, <50% of the islet infiltrated (score 2); and severe insulitis, ≥50% of the islet area infiltrated (score 3), as described (14). Digital images were taken at ×40 magnifications using a Nikon Photomicroscope Eclipse 200. The

Table 1. *Genes and primer sets*

Gene	RefSeq No.	Forward Primer (5′-3′)	Reverse Primer (3′-5′)
Cxcl1	NM_008176	GCACCCAAACCGAAGTCATA	TGTCAGAAGCCAGCGTTCA
Gcg	NM_008100	CTACACCTGTTCGCAGCTCA	CTGGGGTTCTCCTCTGTGTC
Ins1	NM_008386	AAGCTGGTGGGCATCCAGTAACC	GTTTGGGCTCCCAGAGGGCAAG
Ins2	NM_008387	TACACACCCATGTCCCGCCGT	TTCTGCTGGGCCACCTCCAGT
Mafa	NM_194350	GAGGAGGTCATCCGACTGAAA	GCACTTCTCGCTCTCCAGAAT
Nes	NM_016701	AGCAACTGGCACACCTCAA	GGTATTAGGCAAGGGGGAAG
Pdx1	NM_008814	GCTCACGCGTGGAAAGGCCAGGA	CTCTCGGTCAGGTTCAACATCACTGCCAGCT
Pecam1	NM_001032378	CAAGGCCAAACAGAAACCCG	GCTCAAGGGAGGACACTTCC
Ppib	NM_011149	GGAGATGGCACAGGAGGAAA	CCGTAGTGCTTCAGTTTGAAGTTCT
Ppy	NM_008918	CAGGCGACTATGCGACACC	CAGGGAATCAAGCCAACTGG
Reg1	NM_009042	AAGACACCTTGGTCTCAGCC	GCCAGCGACGATTCCTTTTG
Reg2	NM_009043	CACTGCCAACCGTGGTTAT	GACAAAGGAGTACTGTGCCTCA
Sst	NM_009215	CCACCGGGAAACAGGAAC	GCTCCAGCCTCATCTCGTC

Cxcl1, C motif ligand-1 cytokine; Gcg, proglucagon; Ins1 and -2, preproinsulin 1 and 2, respectively; Mafa, v-Maf musculoaponeurotic fibrosarcoma oncogene family, protein A; Nes, nestin (neuroectodermal stem cell marker); Pdx1, pancreatic and duodenal homeobox 1; Pecam1, platelet endothelial cell adhesion molecule-1; Ppib, cyclophilin B; Ppy, pancreatic polypeptide; Reg1 and -2, regenerating genes 1 and 2, Sst, somatostatin.

microscope operator was blinded for the treatments when scoring for insulitis. Insulitis index was calculated as described (31)

$$\text{Insulitis index} = \left[(0 \times n_0) + (1 \times n_1) + (2 \times n_2) + (3 \times n_3)\right] / \left[3 \times (n_0 + n_1 + n_2 + n_3)\right],$$

where n_0, n_1, n_2, and n_3 are the number of islets scored in grades 0, 1, 2 and 3 respectively.

Cytokine Profile

A set of seven cytokines related to Th1 (IFNγ, IL-2, and TNF), Th2 (IL-4, IL-6, and IL-10), and Th17 (IL-17A) immune responses was measured using the Becton Dickinson Th1-Th2-Th17 CBA kit [BD Cytometric Bead Array (CBA) Mouse Th1/Th2/Th17 Cytokine Kit, catalog no. 560485; BD Biosciences, San Jose, CA] in serum samples obtained at euthanization in both experimental designs ($n = 4–8$).

Endocrine Pancreas Histological and Morphometric Analysis

Double staining for glucagon and insulin. Four sections (5 μm) from different regions of the pancreas from each animal were used for double staining with anti-insulin and anti-glucagon antibodies in both the long-term ($n = 4–6$/group) and short-term experimental designs ($n = 4–6$/group). Slides were first overnight (ON) incubated with rabbit anti-glucagon antibody (SC 13091, 1:300; Santa Cruz Biotechnology, Santa Cruz, CA), followed by secondary antibody (biotinylated goat anti-rabbit IgG, BA-1000, 1:200; Vector Laboratories, Burlingame, CA) and Vectastain ABC kit (PK-6100; Vector Laboratories) and 3,3′-diaminobenzidine (DAB; Roche, Mannheim, Germany). Insulin was detected with guinea pig anti-insulin antibody (ON incubation, I8510, 1:300; Sigma-Aldrich), followed by a secondary antibody (biotinylated goat anti-guinea pig IgG, Vector BA-7000, 1:200) and alkaline phospha-

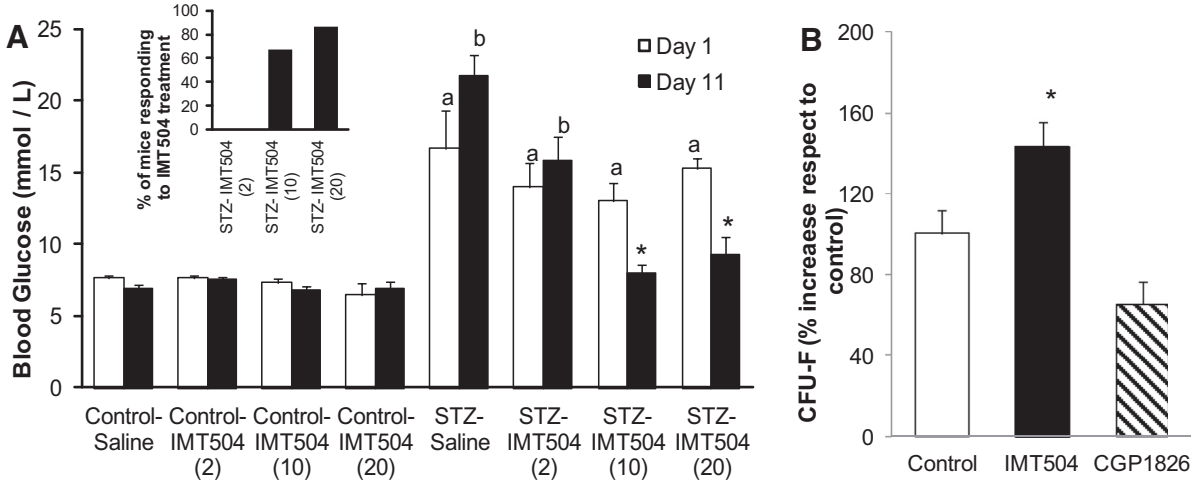

Fig. 1. Preliminary studies. IMT504 dose-response study on blood glucose in multiple low (subdiabetogenic) doses of streptozotocin (MLDS) mice. Effect of IMT504 on in vitro mouse bone marrow (BM)-mesenchymal stem cell (MSC) fibroblast colony-forming unit (CFU-F) formation. *A*: IMT504 dose-response study: 2, 10, or 20 mg/kg IMT504 were injected subcutaneously (sc) daily to MLDS (glycemia ≥12 mM) and control mice for 10 days. Glycemia was measured on *day 1*, before IMT504 treatment started, and on *day 11*, 1 day after the last IMT504 dose. Both 10 and 20 mg/kg IMT504 significantly lowered blood glucose, repeated-measures 2-way ANOVA. Factors: treatment days; interaction: $P < 0.001$. [a]Different from controls on *day 1*, $P < 0.02$; [b]different from controls on *day 11*, $P < 0.001$; *different from *day 1* in the same group, $P < 0.01$. *Inset*: %animals responding to treatment; none of the 2 mg/kg IMT504-injected MLDS mice responded to treatment (0 of 7 = 0%), whereas both 10 (4 of 6 = 67%) and 20 mg/kg (6 of 7 = 86%) showed a satisfactory response to treatment, without significant differences between them. χ^2: %animals responding to 10 vs. 20 mg/kg: not significant (NS). *B*: effect of IMT504 on in vitro mouse BM-MSC CFU-F formation. No. of colonies was counted in each culture treated with PBS (controls), and this was considered 100% for each experiment. %Variation with regard to controls in each experiment was calculated for each stimulus. IMT504 significantly increased the %response. ANOVA: $P < 0.05$. *Significantly different from control and CpG 1826, $P < 0.03$. No. of experiments = 12.

tase Vectastain ABC-AP kit (Vector AK-5000) combined with Vector red substrate (Vector SK-5100). Negative controls were used for assaying nonspecific staining. Sections were mounted on aqueous medium without counterstain. Digital images were taken at ×10 and ×40 magnifications using a Nikon Photomicroscope Eclipse 200. Image analysis was performed with NIS-Elements BR 2.30 software.

Total pancreas area for each section was determined in microphotographs covering all the pancreas sections. Islet number and total islet area, both of which are relative to square millimeters of total pancreas area, were calculated. Glucagon-positive and insulin-positive areas per islet area were also calculated. Data from sections of the same slide were averaged.

Second Experimental Design: Short-Term Effects of IMT504 in Diabetic Mice

With the aim of establishing the early mechanisms by which IMT504 elicits reversion of the diabetic state, MLDS mice (blood glucose ≥12 mM) and control mice were treated daily with IMT504 or poly C ODN (a control for specificity, 20 mg/kg body wt sc), and blood glucose was monitored every day. STZ-IMT504 mice were euthanized after two consecutive decreases in blood glucose in each animal. The number of IMT504 injections per animal to obtain this result in glycemia varied between two and six. Groups of control-saline, control-IMT504, STZ-poly C, and STZ-saline animals were euthanized at the same time as STZ-IMT504 animals. After the nonfasted blood glucose levels were determined, mice were fasted for 3 h, blood glucose was measured, they were then anesthetized with avertin (as above), a transcardiac blood sample was obtained (for serum insulin and cytokines determinations), and they were then euthanized by transcardiac perfusion with 0.9% saline followed by 4% paraformaldehyde in PBS, pH 7.4. Pancreases were excised and processed for immunohistochemical analysis ($n = 4–6$).

Blood glucose, serum insulin, HOMA-IR and HOMA-β-cell, leukocyte infiltration, and cytokine profile were performed as stated above.

Pancreas Histological and Morphometric Analysis

Double staining for glucagon and insulin was performed as described above.

Double staining for PCNA and insulin. Two sections (5 μm) from different regions of each pancreas were used for the double staining with insulin and proliferating cell nuclear antigen (PCNA) in animals from the short-term experimental design ($n = 4–6$/group). For PCNA, tissues were blocked for 1 h with PBS-2% BSA supplemented with 5% goat serum and later incubated ON with rabbit anti-PCNA antibody (1:200 in PBS-2% BSA, sc-7907; Santa Cruz Biotechnology, Dallas, TX) at 4°C. Incubation with 1:200 secondary antibody (goat biotinylated anti-rabbit IgG, BA-1000; Vector Laboratories) lasted for 1 h at room temperature. Slides were then incubated with the Vectastain ABC-AP Kit (AK-5000; Vector Laboratories), and the Vector Blue substrate kit (SK-5300; Vector Laboratories) was then used for staining. Insulin staining was performed as above.

The number of PCNA positive β-cells and PCNA positive non-β-cells/islet were calculated.

Apoptosis evaluation. The apoptotic cells were evaluated using a DeadEnd Fluorometric TUNEL System commercial kit (G3250; Promega) according to the manufacturer's protocol (green staining) in sections of pancreases of the short-term experimental design. We used 1 μg/ml DAPI for 5 min at room temperature in the dark as a nuclear stain (blue staining) and rabbit anti-glucagon antibody (1:300) followed by anti-rabbit IgG (H + L)-Texas Red (red staining; Vector Laboratories) to identify α-cells. Immediately, the samples were analyzed under a confocal microscope to view the green and red fluorescence at 520 ± 20 nm and >620 nm, respectively. The number of apoptotic islets/total islets and the number of apoptotic nuclei per islet were calculated ($n = 4–6$).

Triple immunostaining for Pdx1 or Nkx6.1 together with insulin and glucagon. Insulin was determined as described above. Glucagon were detected as above but followed by the Vectastain ABC-AP Kit combined with the Vector blue AP Kit. Pdx1 was identified with mouse anti-Pdx1 antibody [1:50 ON at 4°C; F109-D12 was deposited to the Developmental Studies Hybridoma Bank (DSHB) by Dr. O. D. Madsen, University of Iowa, Iowa City, IA], and Nkx6.1 was identified with mouse anti-Nkx6.1 antibody (1:50 ON at 4°C; F55A10 was deposited to the DSHB by Dr. O. D. Madsen), followed by 1:100 secondary antibody (horse biotinylated anti-mouse IgG, BA-2000; Vector Laboratories) for 1 h at room temperature; both were revealed with Vectastain ABC Kit and DAB.

The number of Pdx1+ or Nkx6.1+ α- and β-cells per positive islets were calculated ($n = 4–6$).

Immunostaining for indoleamine 2,3-dioxygenase and TSG-6. Pancreas sections were incubated with rabbit anti-indoleamine 2,3-dioxygenase (IDO; sc-25809, 1:100, ON at 4°C; Santa Cruz Biotechnology) or rabbit anti-TSG-6 (sc-30140, 1:100, ON at 4°C; Santa Cruz Biotechnology) antibodies and the corresponding second antibody (goat biotinylated anti-rabbit IgG, 1:200, BA-1000 Vector Labs), which was revealed with DAB, and then counterstained with hematoxylin. IDO- or TSG-6-positive islets per total islets were calculated ($n = 4–6$).

Islet Isolation, RNA Extraction, and Gene Expression Assays

Pancreatic islets were isolated from mice of the second experimental design, as described previously with minor modifications (4).

Fig. 2. First experimental design. Glucose metabolism and islet morphology. *A*: glycemia evolution. Nonfasting blood glucose was evaluated for 66 days in control-saline (◆), control-IMT504 (●), streptozotocin (STZ)-saline (▲), and STZ-IMT504 (■) mice; Arrows indicate IMT504 treatment (20 doses). IMT504 treatment lowered blood glucose significantly in diabetic mice, repeated-measures 2-way ANOVA. Factors: treatment-days; interaction: $P < 0.001$. [a]STZ-saline, different from control-saline and control-IMT504, $P < 0.01$; [b]STZ-IMT504, different from STZ-saline, $P < 0.01$; [c]STZ-IMT504, different from control-saline, $P < 0.01$. *B*: fasted glycemia was determined on *day 60* during the intraperitoneal glucose tolerance test (IPGTT). IMT504 decreased blood glucose to control levels; ANOVA, $P < 0.001$. #Different from all, $P < 0.05$. *C*: fasted serum insulin was determined on *day 60* during the IPGTT. No differences were observed among groups; ANOVA, NS. *D*: HOMA-β-cell was calculated with fasted blood glucose and fasted serum insulin determined on *day 60*. IMT504 normalized this parameter; ANOVA, $P < 0.05$. *Different from all, $P < 0.05$. *E*: homeostasis model assessment of insulin resistance (HOMA-IR) was calculated with fasted blood glucose and fasted serum insulin determined on *day 60*. IMT504 partially reverted this parameter, as it was not significantly different from either controls or STZ-saline; ANOVA, $P < 0.01$; *Different from control-saline and control-IMT504, $P < 0.05$. *F*: IPGTT; glucose (2 g/kg ip) excursion curves were evaluated for all groups. IMT504 partially improved this parameter, as it was able to control glucose overload up to 30 min; repeated-measures 2-way ANOVA. Factors: treatment/time; interaction: $P < 0.001$. [a]Different from all, $P < 0.05$; [b]different from controls, $P < 0.05$; [c]different from controls, $P < 0.01$. *G*: area under the curve (AUC) IPGTT; the area under the glucose curve was calculated. IMT504 decreased this parameter significantly in diabetic mice with respect to STZ-saline, albeit not attaining control levels; ANOVA, $P < 0.001$. *STZ-saline, different from all, $P < 0.04$; #STZ-IMT504, different from all, $P < 0.04$. Representative images of insulin (red) and glucagon (brown) double-stained islets; magnification, ×400. *H*: islet no./mm^2 pancreas was calculated for all groups. STZ-saline induced a decreased in islet number that was reversed by IMT504; ANOVA, $P < 0.01$. *Different from all, $P < 0.01$. *I*: islet area/mm^2 pancreas was calculated for all groups. STZ-saline induced a decrease in islet area with regard to control that was partially reversed by IMT504; ANOVA, $P < 0.01$. *Different from control-saline and control-IMT504, $P < 0.05$. *J*: glucagon-positive (black bars) and insulin-positive (open bars) areas/islet area were calculated for all groups. Glucagon area did not vary among groups; ANOVA, NS. Insulin area was decreased in STZ-saline islets and partially recovered by IMT504 treatment; ANOVA, $P < 0.001$. *Different from all, $P < 0.05$.

Briefly, we injected 3 ml of a liberase solution into the pancreatic duct in anesthetized mice (Liberase TL Research Grade, 05401020001, Roche; commercialized by Sigma-Aldrich, which was dissolved in RPMI medium; RPMI, 31800022; Gibco, Carlsbad, CA). The liberase concentration was 0.155 mg/ml. The pancreas was then gently removed for its further digestion in liberase solution at 37°C for 14 min in a 50-ml Falcon tube. The digestion was stopped by 40 ml of ice-cold RPMI 1640 supplemented with 10% FBS. Islets were hand-picked under a dissecting microscope into fresh RPMI-10% FBS and then hand-picked for a second time into TRIzol reagent (Invitrogen, Carlsbad, CA) and homogenized for further RNA extraction.

Total RNA was isolated from TRIzol homogenates according to the manufacturer's protocol and kept at −70°C until being purified further with a NucleoSpin RNA kit (Macherey-Nagel, Bethlehem, PA); 0.5 μg

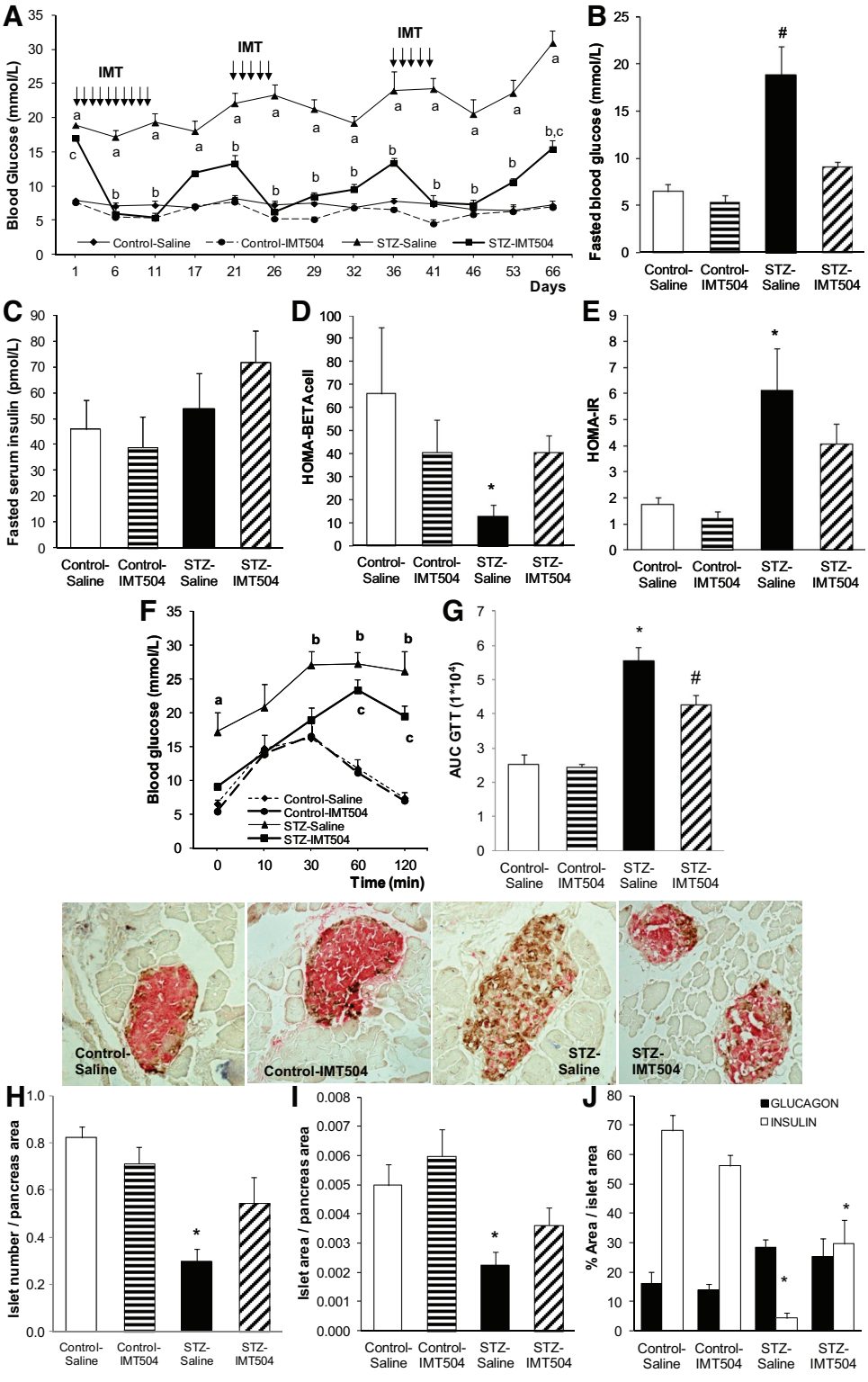

of RNA was reverse-transcribed in a 20-μl reaction using MMLV reverse transcriptase (Epicentre, Madison, WI) and oligo(dT) 15 primers (Biodynamics, Buenos Aires, Argentina). The reverse transcriptase was omitted in control reactions, where the absence of an amplification product indicated the isolation of RNA free from genomic DNA.

For quantitative real-time PCR, primer sets were chosen for the specific amplification of the following murine genes: preproinsulin 1 (*Ins1*), preproinsulin 2 (*Ins2*), proglucagon (*Gcg*), pancreatic polypeptide (*Ppy*), somatostatin (*Sst*), pancreatic and duodenal homeobox 1 (*Pdx1*), v-Maf musculoaponeurotic fibrosarcoma oncogene family, protein A (*MafA*), platelet endothelial cell adhesion molecule (*Pecam1*; also known as cluster of differentiation 31), regenerating genes 1 and 2 (*Reg1* and *Reg2*), nestin (neuroectodermal stem cell marker) (*Nes*), C-X-C motif ligand 1 cytokine (*Cxcl1*), and cyclophilin B (*Ppib*) as the housekeeping control gene (Table 1).

Target cDNA quantification was performed by kinetic PCR in a total volume of 10 μl using 5 × HOT FIREPol EvaGreen qPCR Mix Plus (Solis BioDyne, Tartu, Estonia) according to the manufacturer's protocol, with an additional annealing step. Amplification was carried out in an ABI 7500 sequence detection system (Applied Biosystems, Carlsbad, CA). Results were validated based on the quality of the dissociation curves, and the product purity was confirmed by 2.3% agarose gel electrophoresis. Each sample was analyzed in duplicate along with nontemplate controls to monitor nucleic acid contamination.

Quantitative differences in the cDNA target between samples were determined using the mathematical model of Pfaffl, as described previously ($n = 5–6$) (9).

Statistical Analysis

Results are expressed as means ± SE. Differences between means were analyzed by one-way ANOVA, followed by post hoc tests; for multiple determinations in the same animal, we used two-way ANOVA with repeated-measures design (Statistica Release 7). Differences in percentages between two groups were analyzed with the χ^2 test; when more than two groups were compared, the data were arcsine transformed and analyzed by ANOVA. In all cases, $P < 0.05$ was considered significant.

RESULTS

Preliminary Studies

Preliminary tests were performed to confirm the biological effect and determine the optimal dose of IMT504 in MLDS mice. Moreover, its effect on in vitro mouse MSC proliferation was also analyzed.

Dose-Response Study

Both 10 and 20 mg/kg IMT504 lowered blood glucose in MLDS mice significantly, whereas 2 mg/kg was ineffective (repeated-measures 2-way ANOVA, interaction $P < 0.001$, STZ-IMT504 10 mg/kg: *day 11* vs. *day 1*, $P < 0.01$; STZ-IMT504 20 mg/kg: *day 11* vs. *day 1*, $P < 0.01$; Fig. 1*A*). The percentage of animals responding to treatment increased with 20 (6 of 7) vs. 10 mg/kg (4 of 6), albeit not significantly (NS; 86 vs. 67%, χ^2; Fig. 1*A*, *inset*), whereas none of the 2 mg/kg injected animals responded to treatment (0/7). We selected 20 mg/kg as the optimal dose for treatment in mice.

In Vitro Mouse BM-MSC CFU-F Formation

IMT504 increased the number of CFU-Fs of mouse BM cells significantly compared with controls (ANOVA: $P < 0.05$,

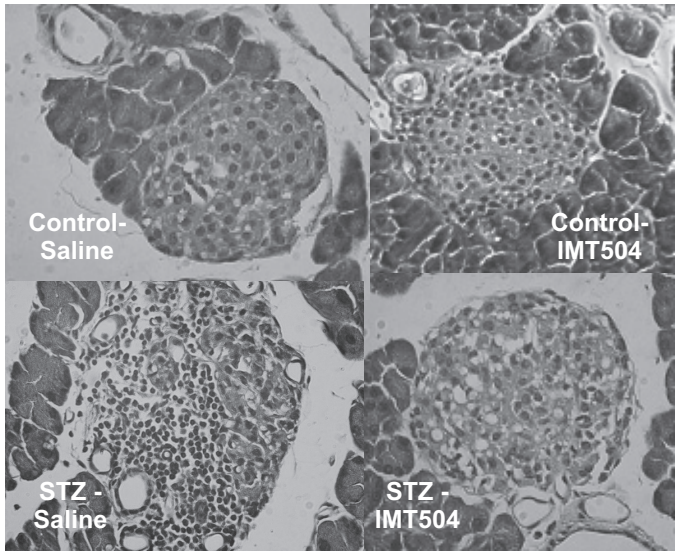

A LEUCOCYTE INFILTRATION

	ISLETS IN EACH CATEGORY (%MOUSE)			
TREATMENT	0	1	2	3
Control-Saline	91.1±4.5	8.9±4.5	0	0
Control-IMT504	88.4±0.5	11.6±0.5	0	0
STZ-Saline	5.6±5.6	16.7±9.6	50.0±0.0	24.8±11.1
STZ-IMT504	52.8±9.7	31.9±3.7	11.6±6.4	3.7±3.7

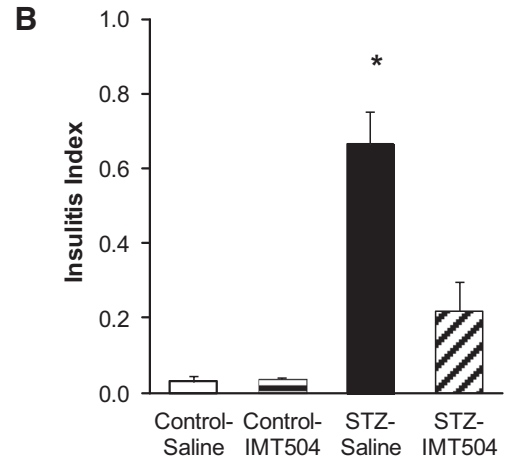

Fig. 3. First experimental design. Immune parameters. Representative photomicrographs of hematoxylin-stained sections; magnification, ×400. *A*: insulitis scores in Langerhans islets. Insulitis scoring was evaluated according to the following criteria: no insulitis (score 0); peri-insulitis, insulitis restricted to the periphery of islets (score 1); moderate insulitis, <50% of the islet infiltrated (score 2); and severe insulitis, ≥50% or higher of the islet area infiltrated (score 3). %Islets in each category was calculated for all of the experimental groups. *B*: insulitis index was calculated as follows: insulitis index = $[(0 \times n_0) + (1 \times n_1) + (2 \times n_2) + (3 \times n_3)]/[3 \times (n_0 + n_1 + n_2 + n_3)]$, where n_0, n_1, n_2, and n_3 are the nos. of islets scored in grades 0, 1, 2, and 3, respectively. IMT504 reduced the insulitis index significantly in STZ-IMT504 mice; ANOVA, $P < 0.001$. *Different from all, $P < 0.001$.

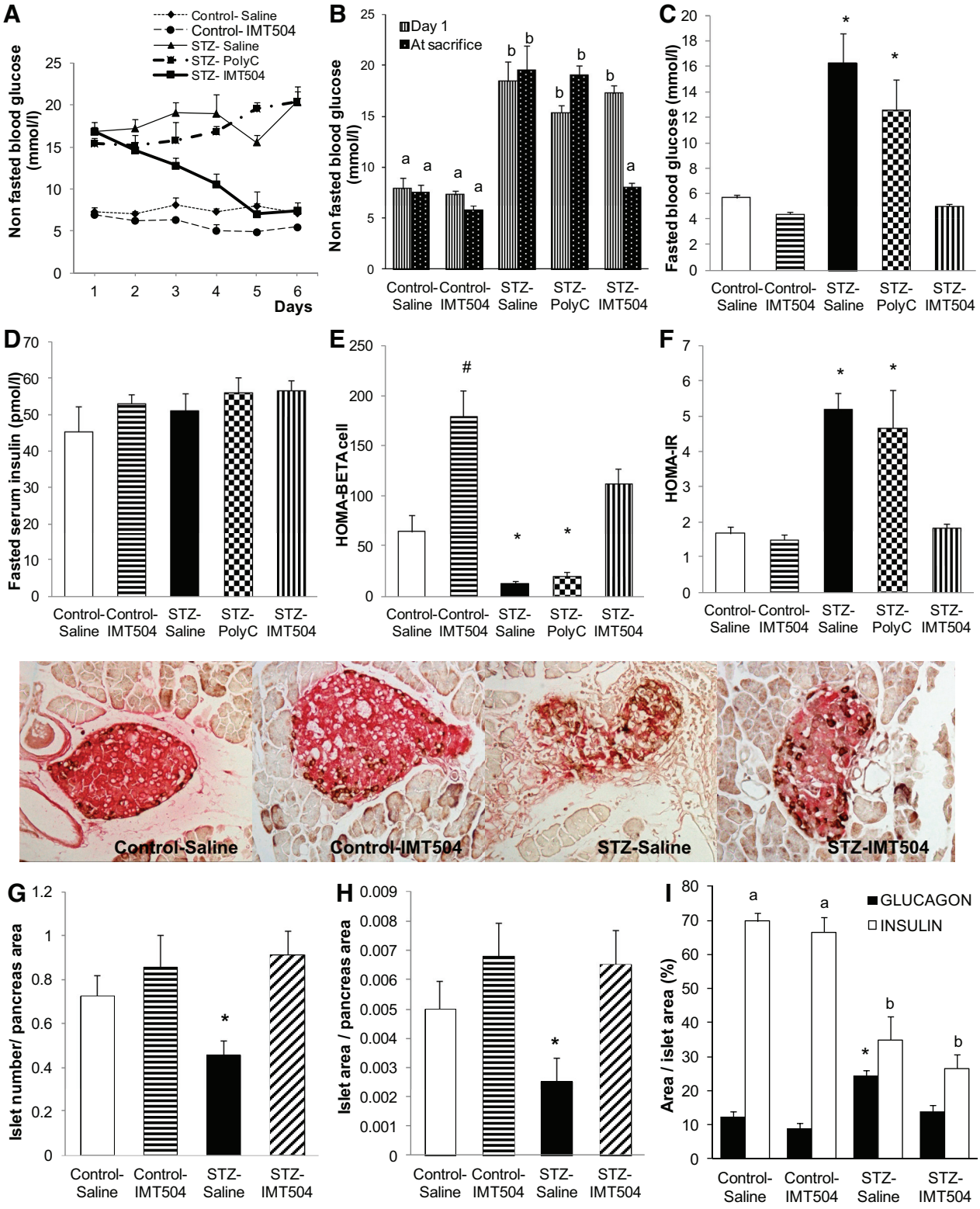

IMT504 vs. control and CpG 1826, $P < 0.03$; Fig. 1*B*). In contrast, CpG ODN 1826, a specific mouse TLR9 agonist, had no effect.

First Experimental Design: Long-Term Effect of IMT504 in MLDS Mice

Once the optimal dose was determined, the long-term effect of IMT504 was confirmed by a set of parameters that included functional pancreatic tests, islet morphology, and leukocyte infiltration.

Glucose metabolism and islet morphology. Blood glucose levels were similar in all mice at the time of them being assigned to the diabetic (MLDS) or control (vehicle-injected) groups (nonfasted blood glucose: control-saline = 8.3 ± 0.7, control-IMT504 = 8.0 ± 0.6, STZ-saline = 8.0 ± 0.4, STZ-IMT504 = 7.6 ± 0.6, ANOVA; NS).

After 15–20 days of MLDS treatment, mice developed hyperglycemia (Fig. 2*A*), and IMT504 treatment, or saline as control, was commenced (*day 1*). Blood glucose increased progressively in STZ-saline mice during 10 wk of evaluation, whereas it decreased significantly in STZ-IMT504 mice (repeated-measures 2-way ANOVA, interaction $P < 0.001$, STZ-IMT504 different from STZ-saline on *days 6*, *11*, *21*, *26*, *29*, *32*, *36*, *41*, *46*, *53*, and *66*, $P < 0.01$ or less; Fig. 2*A*). Eighty-eight percent of STZ-IMT504 animals responded to treatment (7 of 8), whereas 20% of STZ-saline mice (2 of 10) showed spontaneous diabetes reversion (χ^2: $P < 0.025$). The graphs in Fig. 2, *B–J*, show data of STZ-IMT504 responding animals. The first five IMT504 doses sufficed to normalize glycemia. However, after drug interruption, a gradual increase in blood glucose occurred that was normalized upon reinitiating IMT504 treatment. At the end of the experiment (*day 66*), 26 days after the last IMT504 dose, blood glucose was significantly lower in STZ-IMT504 than in diabetic mice, albeit higher than in controls (repeated-measures 2-way ANOVA, interaction $P < 0.001$; *day 66*: STZ-IMT504 vs. control-saline, control-IMT504, and STZ-saline, $P < 0.01$).

Body weight was determined in these mice on the 1st day of each treatment, when the first dose of STZ was administered and when the first dose of each IMT504 cycle was administered (*days 1*, *21*, and *36*) and also on the day of euthanization (*day 66*). We did not observe any significant differences in body weight due to IMT504 treatment in either controls or MLDS-treated mice (not shown).

IPGTT was performed 20 days after the last IMT504 dose. Fasted blood glucose in STZ-IMT504 mice was similar to controls and significantly lower than in STZ-saline (ANOVA, $P < 0.001$; STZ-IMT504 vs. STZ-saline, $P < 0.05$; Fig. 2*B*). Fasted serum insulin was similar among groups (ANOVA: NS) (Fig. 2*C*). HOMA indexes derive from relationships between fasted blood glucose and serum insulin levels and are used here as an approximation to insulin secretion and action. IMT504 normalized β-cell function (ANOVA, $P < 0.05$, STZ-saline vs. control-saline, control-IMT504, and STZ-IMT504, $P < 0.05$, HOMA-β-cell; Fig. 2*D*) and improved insulin resistance (ANOVA, $P < 0.01$, STZ-saline vs. control-saline and control-IMT504, $P < 0.05$, HOMA-IR; Fig. 2*E*). The glucose excursion was severely impaired in STZ-saline mice (Fig. 2*F*) and improved by IMT504, which also significantly decreased the area under the glucose curve (ANOVA, $P < 0.001$, STZ-IMT504 vs. control-saline, control-IMT504, and STZ-saline, $P < 0.04$; Fig. 2*G*).

Islet number/pancreas area (Fig. 2*H*) and islet area/pancreas area (Fig. 2*I*) in STZ-IMT504 mice did not differ from controls, demonstrating at least partial recovery, whereas both decreased significantly in diabetics (islet number/pancreas area: ANOVA, $P < 0.01$, STZ-saline vs. control-saline, control-IMT504, and STZ-IMT504, $P < 0.01$; islet area/pancreas area: ANOVA $P < 0.01$, STZ-saline vs. control-saline and control-IMT504, $P < 0.05$). Additionally, STZ induced a significant decrease in β-cell area (Fig. 2*J*) that reversed significantly with IMT504, albeit not attaining control levels (ANOVA, $P < 0.001$, STZ-IMT504 vs. control-saline, control-IMT504, and STZ-saline, $P < 0.05$).

Immune parameters. MLDS mice showed marked insulitis (Fig. 3*A*); this was significantly reversed by IMT504 (Fig. 3*B*), demonstrating effective inhibition of leukocyte infiltration even after 26 days without treatment (insulitis index: ANOVA, $P < 0.001$, STZ-saline vs. control-saline, control-IMT504, and STZ-IMT504, $P < 0.001$). Circulating cytokines did not differ among groups (not shown).

Second Experimental Design: Short-Term Effect of IMT504 in MLDS Mice

Taking into account that IMT540 showed significant, long-lasting improvement in immunodependent diabetes, we studied its effect shortly after treatment initiation when the regenerative process was commencing.

Glucose metabolism and islet morphology. MLDS mice were treated daily with 20 mg/kg IMT504 and euthanized after two consecutive drops in blood glucose. A group of MLDS mice was treated similarly with a poly C ODN, with the same

Fig. 4. Second experimental design. Glucose metabolism and islet morphology. *A*: nonfasted glycemia evolution; MLDS mice (blood glucose ≥12 mM) and control mice were treated daily with 20 mg/kg IMT504 or poly C oligonucleotides (ODN; a control for specificity, 20 mg/kg body wt sc), and blood glucose was monitored every day. STZ-IMT504 mice were euthanized after 2 consecutive decreases in blood glucose in each animal. The no. of IMT504 injections/animal to obtain this result in glycemia varied between 2 and 6. *B*: nonfasted glycemia before treatment initiation and at euthanization in each animal. IMT504 significantly lowered blood glucose to control levels, whereas poly C ODN had no effect; repeated-measures 2-way ANOVA, interaction $P < 0.001$. Different letters indicate significant differences, $P < 0.001$. *C*: fasted glycemia at euthanization. IMT504 significantly normalized fasted blood glucose in STZ-IMT504 mice, whereas poly C ODN had no effect; ANOVA, $P < 0.001$. *Different from all, $P < 0.001$. *D*: fasted serum insulin at euthanization did not differ among groups; ANOVA, NS. *E*: HOMA-β-cell. IMT504 normalized this parameter in STZ-IMT504 mice; ANOVA, $P < 0.001$. *Different from control-saline, control-IMT504, and STZ-IMT504, $P < 0.01$; #different from control-saline, STZ-saline, and STZ-Poly C, $P < 0.04$. *F*: HOMA-IR. This parameter was normalized in STZ-IMT504 mice; ANOVA, $P < 0.001$. *Different from controls and STZ-IMT504, $P < 0.001$. Representative images of insulin (red) and glucagon (brown) double-stained islets. *G*: islet no./mm^2 pancreas. Islet no./mm^2 tended to decrease in STZ-saline mice and was restored by IMT504 in diabetic mice; ANOVA, $P < 0.01$. *Different from control-IMT504 and STZ-IMT504, $P < 0.03$. *H*: islet area/mm^2 pancreas. Islet area/mm^2 tended to decrease in STZ-saline mice and was restored by IMT504 in diabetic mice ANOVA, $P < 0.05$. *Different from control-IMT504 and STZ-IMT504, $P < 0.02$. *I*: insulin-glucagon area/islet area (%); insulin area decreased in both STZ-saline and STZ-IMT504 islets; ANOVA, $P < 0.001$. [a,b]Different from each other, $P < 0.01$. Glucagon area increased in STZ-saline islets and was normalized by IMT504; ANOVA, $P < 0.001$, *Different from all, $P < 0.01$.

phosphorothioate backbone and length (20 mg/kg), to test the specificity of the IMT504 response. Nonfasted saline-treated diabetic mice were hyperglycemic; in contrast, two to six doses of IMT504 significantly lowered glycemia to control levels (Fig. 4, *A* and *B*), whereas poly C ODN was ineffective (repeated-measures 2-way ANOVA, interaction $P < 0.001$, STZ-IMT504, blood glucose at euthanization vs. on *day 1*, $P < 0.001$).

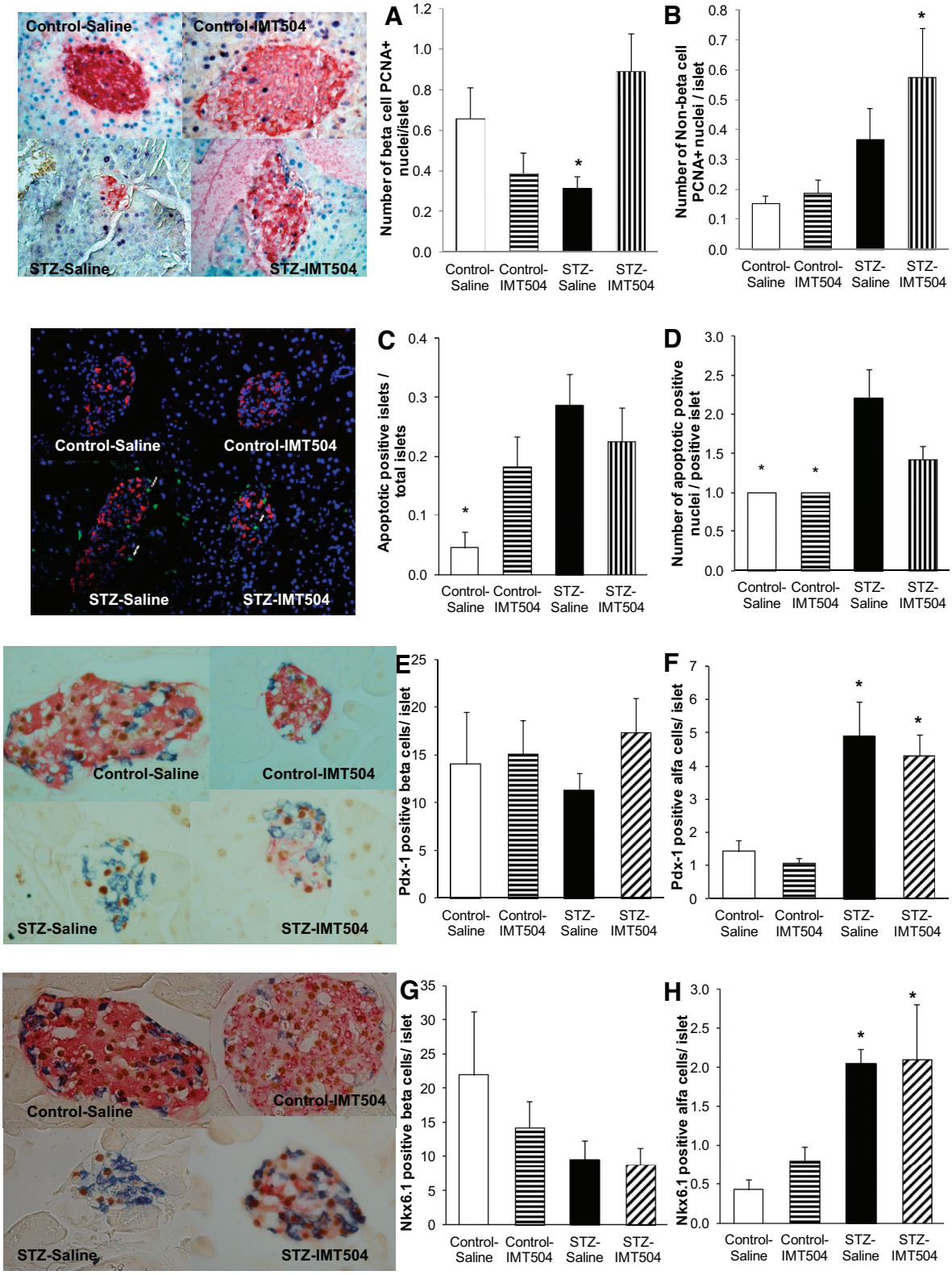

After 3 h of fasting, blood glucose showed the same pattern as in nonfasted mice (ANOVA: $P < 0.001$, STZ-saline and STZ-poly C vs. control-saline, control-IMT504, and STZ-IMT504, $P < 0.001$; Fig. 4*C*). Fasted insulin did not vary among groups (ANOVA: NS; Fig. 4*D*). HOMA-β-cell (Fig. 4*E*) and HOMA-IR (Fig. 4*F*) were normalized by IMT504 but not by poly C ODN (HOMA-β-cell, ANOVA: $P < 0.001$, STZ-saline and STZ-poly C vs. control-saline, control-IMT504, and STZ-IMT504, $P < 0.01$; HOMA-IR, ANOVA: $P < 0.001$, STZ-saline, and STZ-poly C vs. control-saline, control-IMT504, and STZ-IMT504, $P < 0.001$).

Islet number/pancreas area (Fig. 4*G*) and islet area/pancreas area (Fig. 4*H*) decreased in STZ-saline and were normalized by IMT504 (islet number/pancreas area, ANOVA: $P < 0.01$, STZ-saline vs. control-IMT504 and STZ-IMT504, $P < 0.03$; islet area/pancreas area, ANOVA: $P < 0.05$, STZ-saline vs. control-IMT504 and STZ-IMT504, $P < 0.02$). β-Cell area/islet area decreased in STZ-saline and STZ-IMT504 (ANOVA: $P < 0.001$, STZ-saline and STZ-IMT504 vs. control-saline and control-IMT504, $P < 0.01$), whereas α-cell area/islet area increased in STZ-saline and reversed with IMT504 (ANOVA, $P < 0.001$, STZ-saline vs. control-saline, control-IMT504, and STZ-IMT504, $P < 0.01$; Fig. 4*I*).

Proliferation, apoptosis, and progenitor cell markers. STZ induced a near-significant ($P < 0.07$) decrease in β-cell proliferation. Conversely, PCNA+ nuclei/islet increased significantly in STZ-IMT504 mice in both β- and non-β (presumably α)-cells [no. of PCNA+ β-cells/islet, ANOVA: $P < 0.02$, STZ-IMT504 vs. STZ-saline, $P < 0.05$ (Fig. 5*A*); no. of PCNA+ non-β-cells/islet, ANOVA: $P < 0.05$, STZ-IMT504 vs. control-saline and control-IMT504, $P < 0.03$ (Fig. 5*B*)].

STZ increased apoptosis in islets, likely in β-cells, as α-cells (stained red) did not show apoptosis. IMT504 partially reversed this effect [no. of apoptotic islets/total islets, ANOVA: $P < 0.01$, control-saline vs. STZ-saline, $P < 0.05$ (Fig. 5*C*); no. of apoptotic nuclei/positive islets, ANOVA: $P < 0.05$, control-saline and control-IMT504 vs. STZ-saline, $P < 0.05$ (Fig. 5*D*)].

The total number of Pdx1+ and Nkx6.1+ nuclei/islets did not vary among groups (not shown). Interestingly, the number of Pdx1+ or Nkx6.1+ β-cells did not vary due to treatment (ANOVA: NS) (Fig. 5, *E* and *G*); instead, the diabetic state (STZ-saline and STZ-IMT504) induced a significant increase in Pdx1 and Nkx6.1 expression in α-cells that usually do not express these markers in adulthood [Pdx1, ANOVA: $P < 0.01$, STZ-saline and STZ-IMT504 vs. control-saline and control-IMT504, $P < 0.01$ (Fig. 5*F*); Nkx6.1, ANOVA: $P < 0.05$, STZ-saline and STZ-IMT504 vs. control-saline and control-IMT504, $P < 0.05$ (Fig. 5*H*)].

Immune parameters. MLDS triggered islet leukocyte infiltration. IMT504 significantly reduced infiltration to near-normal levels (Fig. 6*A*). Insulitis index was increased in STZ-saline islets and reversed significantly by IMT504 (Fig. 6*B*) (ANOVA: $P < 0.001$, STZ-saline vs. control-saline, control-IMT504 and STZ-IMT504, $P < 0.01$).

IMT504 induced specific increases in IL-6 and TNF in the control-IMT504 and STZ-IMT504 groups, suggesting IMT504-dependent effects (IL-6, ANOVA: $P < 0.01$, control-IMT504 and STZ-IMT504 vs. control-saline and STZ-saline, $P < 0.04$; TNF, ANOVA: $P < 0.001$, control-IMT504 and STZ-IMT504 vs. control-saline and STZ-saline, $P < 0.05$; Fig. 6*C*); no differences were observed for the other cytokines.

IDO and TSG-6 have anti-inflammatory effects (28, 35). IMT504 induced an increase in IDO expression in diabetic islets, suggesting that this may be one mechanism by which it controls islet infiltration (ANOVA: $P < 0.01$, STZ-IMT504 vs. control-saline and control-IMT504, $P < 0.03$; Fig. 6*D*). Because we detected an increase in TNF in IMT504-treated animals and this cytokine stimulates tumor necrosis factor-inducible gene 6 protein (TSG-6) production, we evaluated its expression, finding no differences due to treatment (not shown).

Islet gene expression. In isolated islets, we evaluated expression of genes encoding for islet hormones, transcription factors, and other proteins that could play a role in β-cell survival, apoptosis, and/or regeneration.

In MLDS islets, we observed increased expression of *Ins2*, *Gcg*, and *Sst* (Fig. 7, *A–C*); IMT504 partially or totally reversed these increases (*Ins2/Ppib*, ANOVA: $P < 0.001$, STZ-saline vs. control-saline, control-IMT504 and STZ-IMT504, $P < 0.04$; *Gcg/Ppib*, ANOVA: $P < 0.001$, STZ-saline vs. control-saline, control-IMT504, and STZ-IMT504, $P < 0.002$; *Sst/Ppib*, ANOVA: $P < 0.02$, STZ-saline vs. control-saline, control-IMT504, and STZ-IMT504, $P < 0.03$).

Ins1 and *Ppy* were unaltered (ANOVA, NS; Fig. 7, *D* and *E*), whereas *Pdx1* and *Mafa* decreased in both STZ-saline and STZ-IMT504 islets, but only *Mafa* attained statistical significance (Fig. 6, *F* and *G*) (ANOVA: $P < 0.04$, control-saline vs. STZ-saline and STZ-IMT504, $P < 0.03$).

Nestin, *Reg1*, and *Cxcl1* increased in STZ-saline islets and were reversed by IMT504 (*Nes/Ppib*, ANOVA: $P < 0.01$, STZ-saline vs. control-saline, control-IMT504, and STZ-IMT504, $P < 0.03$; *Reg1/Ppib*, ANOVA: $P < 0.02$, STZ-

Fig. 5. Second experimental design. Proliferation, apoptosis, and progenitor cell markers. *Left*: representative photomicrographs of islets. *A* and *B*: insulin (red) and proliferating cell nuclear antigen (PCNA; blue). Proliferation of islet cells was evaluated by PCNA staining. *A*: no. of PCNA+ β-cells/islet tended to decrease in STZ-saline islets with regard to controls and increase in STZ-IMT504 islets; ANOVA, $P < 0.02$. *Different from STZ-IMT504, $P < 0.05$. *B*: no. of PCNA+ non-β-cell/islet (presumably α-cells) increased in STZ-IMT504 islets; ANOVA, $P < 0.05$. *STZ-IMT504, different from control-saline and control-IMT504, $P < 0.03$. *C* and *D*: glucagon (red), apoptotic nuclei (green), and other nuclei (blue). Apoptosis in islet cells was evaluated by the TUNEL method. *C*: no. of apoptotic islets/total islets increased in STZ-saline and was partially reversed by IMT504; ANOVA, $P < 0.01$. *Different from STZ-saline, $P < 0.05$. *D*: no. of apoptotic nuclei/positive islet (presumably in β-cells, as α-cells did not show apoptosis) increased in STZ-saline islets and was normalized by IMT504; ANOVA, $P < 0.05$. *Different from STZ-saline, $P < 0.05$. *E* and *F*: insulin (red), glucagon (blue), and Pdx-1 (brown). Expression of pancreatic and duodenal homeobox 1 (Pdx-1), a characteristic marker of adult β-cells, was evaluated in islets from all experimental groups. *E*: no. of Pdx-1+ β-cells/islet did not vary among groups; ANOVA, NS. *F*: no. of Pdx-1+ α-cells/islet increased in STZ-saline and STZ-IMT504 groups; ANOVA, $P < 0.01$. *Different from control-saline and control-IMT504, $P < 0.01$. *G* and *H*: insulin (red), glucagon (blue), and Nkx6.1 (brown). Expression of Nkx6.1, another characteristic marker of adult β-cells, was evaluated in islets from all experimental groups *G*: no. of Nkx6.1+ β-cells/islet did not vary among groups; ANOVA, NS. *H*: no. of Nkx6.1+ α-cells/islet increased in STZ-saline and STZ-IMT504 groups; ANOVA, $P < 0.05$. *Different from control-saline and control-IMT504, $P < 0.05$.

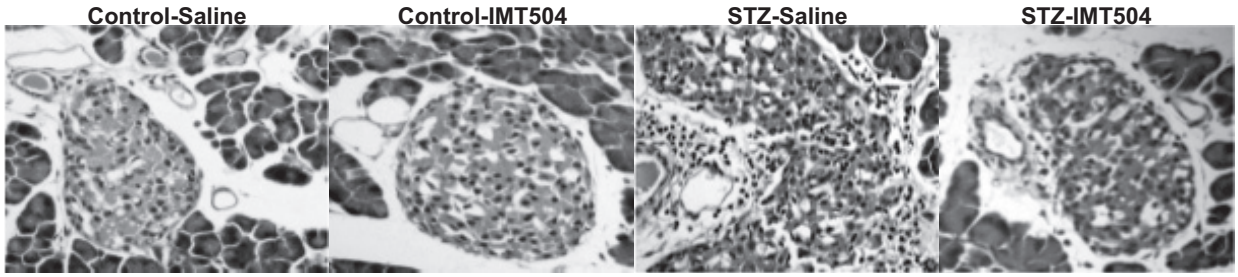

A

LEUCOCYTE INFILTRATION				
	ISLETS IN EACH CATEGORY (%MOUSE)			
TREATMENT	0	1	2	3
Control-Saline	98.0±1.2	2.0±1.2	0	0
Control-IMT504	90.2±3.5	9.8±3.5	0	0
STZ-Saline	37.0±10.1	13.9±4.9	44.6±14.1	4.5±4.5
STZ-IMT504	73.7±5.3	12.7±4.5	13.6±3.9	0

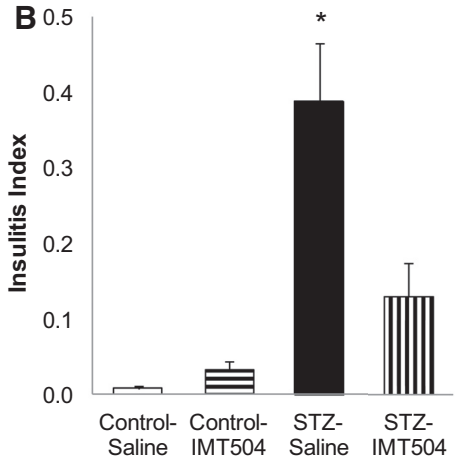

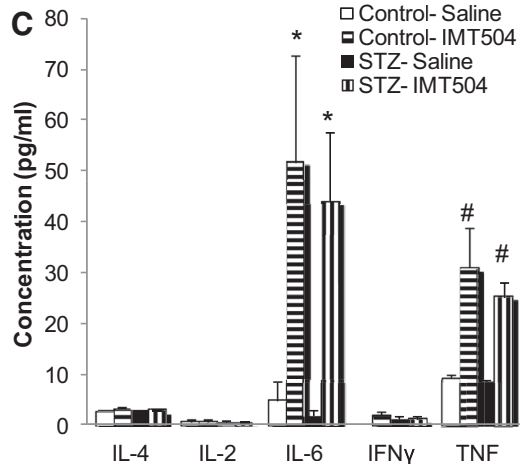

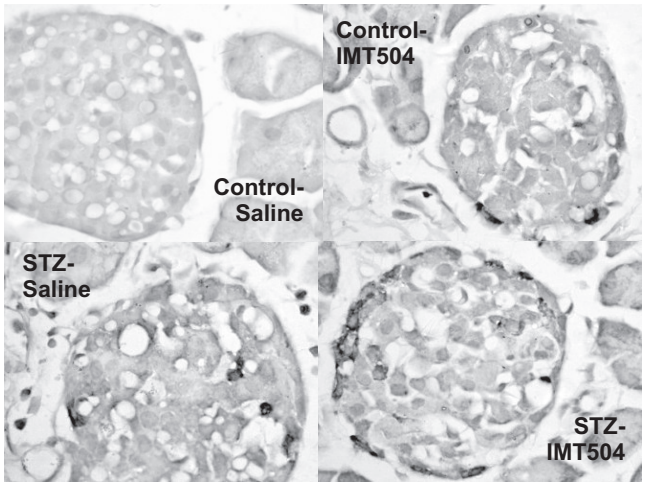

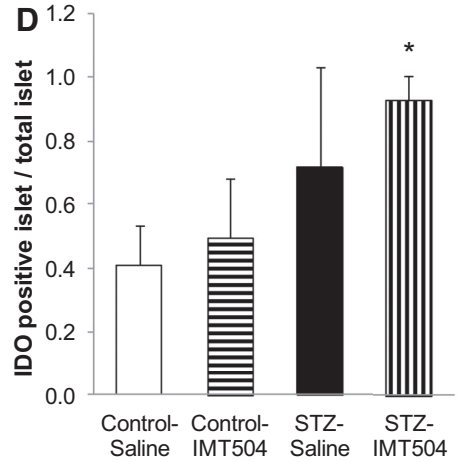

Fig. 6. Second experimental design. Immune parameters. Representative microphotographs of hematoxylin-stained islets. *A*: leukocyte infiltration; percentage in each category. *B*: insulitis index. Insulitis increased in STZ-saline islets and was decreased significantly by IMT504 treatment; ANOVA, $P < 0.001$, *Different from all, $P < 0.01$. *C*: serum cytokines; cytokine levels were evaluated in serum at euthanization in all experimental groups. IL-6 increased in control-IMT504 and STZ-IMT504 mice, indicating that it was an IMT504-dependent effect; ANOVA, $P < 0.01$. *Control-IMT504 and STZ-IMT504, different from control-saline and STZ-saline, $P < 0.04$. TNF increased in control-IMT504 and STZ-IMT504 mice, indicating that it was also an IMT504-dependent effect; ANOVA, $P < 0.001$. #Control-IMT504 and STZ-IMT504, different control-saline and STZ-saline, $P < 0.05$. IL-2, Il-4, and IFNγ; ANOVA, NS. IL-17A and IL-10, nondetectable. Representative microphotographs of indoleamine 2,3-dioxygenase (IDO)-stained islets (brown). *D*: IDO is a protein with anti-inflammatory effects. IDO+ islets/total islets increased in STZ-IMT504 mice; ANOVA, $P < 0.01$. *Different from control-saline and control-IMT504, $P < 0.03$.

saline vs. control-saline and control-IMT504, $P < 0.01$; *Cxcl1/Ppib*, ANOVA: $P < 0.05$, STZ-saline vs. control-saline, control-IMT504, and STZ-IMT504, $P < 0.04$; Fig. 7, *H–J*).

Pecam1 decreased in both control-IMT504 and STZ-IMT504 islets, demonstrating a clear ODN-dependent effect (ANOVA: $P < 0.01$, control-IMT504 and STZ-IMT504 vs. control-saline and STZ-saline, $P < 0.03$; Fig. 7*K*).

Interestingly, *Reg2* significantly increased in STZ-IMT504-treated islets (ANOVA: $P < 0.02$, STZ-IMT504 vs. control-saline and control-IMT504, $P < 0.05$; Fig. 7*L*).

DISCUSSION

Here we evaluated IMT504 as a possible therapy for immunodependent diabetes. We validated its effectiveness in mice by demonstrating its in vitro MSC cloning capacity and its blood glucose-lowering effect in a model of immunodependent diabetes, which was in line with our previous results in rats (3, 22).

Regarding the long-term IMT504 effects, this ODN efficiently lowered blood glucose with an 88% response rate. Although in this diabetes model there is some spontaneous reversion (~20% in our colony) (12), the clear difference in the rate demonstrated the specific effect of IMT504. Glucose metabolism showed marked improvement, consistent with islet recovery. Moreover, insulitis was reduced markedly. In this diabetes model, in which the immune attack is incessant, similar to T1D, a partial increase in blood glucose was observed after IMT504 interruption. Because we did not evaluate food intake in these animals, we acknowledge the possibility that reduced food intake may be a factor in the glucose normalization after IMT504 injections, which will have to be determined in future experiments. Although the glycemic control obtained was considerable, drug administration will have to be perfected to attain a more sustained response.

In the short-term analysis, IMT504 reduced blood glucose to control levels, islet parameters had partially recovered, β-cell apoptosis was inhibited, and proliferation was induced. Nevertheless, the decrease in insulin-positive area persisted even when islet area increased, suggesting that β-cells may not be accumulating enough insulin for its detection by IHC. IMT504 already markedly reduced islet infiltration, demonstrating its immunomodulatory role.

IDO inhibits T cell proliferation, representing an important physiological mechanism controlling both inflammation and autoimmunity (35). Similar to CpG ODNs (14), IMT504 increased IDO expression in islets from diabetic mice, suggesting that this may be one mechanism by which it controls islet infiltration, although this should be confirmed by inhibiting IDO action and thus curtailing IMT504 action. Furthermore, IMT504 increased serum IL-6 and TNF independently of whether the mice were diabetic or not, demonstrating an ODN-associated effect. IL-6 is a pleiotropic cytokine with multiple functions (16) proposed to induce protective actions in the short term, whereas in the long term it may play a role in the pathogenesis of disease (16). Regarding its protective actions, IL-6 modulates the Th1/Th2 balance towards Th2 (11), favors the presence of M2 immunosuppressor macrophages (33), and inhibits the proliferation of CD4+ and CD8+ lymphocytes (15). Moreover, IL-6 inhibits β-cell apoptosis (38). Therefore, IMT504-induced IL-6 increase may be protecting islets from STZ-induced damage by immunosuppressive and proregenerative actions.

TNF is the prototype of proinflammatory cytokines; nevertheless, its pleiotropic effects often lead to opposing outcomes during the development of immune-mediated diseases (39). TNFα can act as an antiapoptotic signal and promote cell survival and proliferation in certain tissues (40). The IMT504-induced increase in circulating TNF may help promote β-cell survival/proliferation while not stimulating inflammation or apoptosis, as β-cell death and islet infiltration were reduced by IMT504. It will be interesting to establish which cells produce IL-6 and TNF in the context of IMT504 stimulation in this diabetes model and the mechanisms by which they may be exerting their beneficial effects. Interestingly, MSCs release IL-6 and IDO, which participate in the anti-inflammatory actions of these cells (15). Taking into account our previous results (3, 22) and the present preliminary results, we hypothesized that IMT504 could potentially stimulate MSCs to participate in tissue repair and immunomodulation in this diabetes model. In vitro IMT504 increased mouse CFU-F formation, which is an indication of self-renewal stimulation of bone marrow mesenchymal progenitors. However, IMT504 did not stimulate nestin mRNA expression, one postulated marker of pancreas progenitors, in the present conditions (46). Nevertheless, the potential participation of pancreatic progenitors stimulated by IMT504 in the recovery of β-cells cannot be discarded and remains to be explored further in future experiments.

Interestingly, Pdx1 and Nkx6.1 expression increased in α-cells in diabetic mice, but not in β-cells, independent of IMT504 treatment, suggesting an early event in α/β-transdif-

Fig. 7. Second experimental design. Gene expression (quantitative PCR), which was evaluated in islets isolated from STZ-IMT504 mice after 2 consecutive decreases in blood glucose. Mice from the other experimental groups were euthanized at the same time. *A*: *Ins2*/*Ppib* increased in STZ-saline islets and significantly reverted to control levels in STZ-IMT504 islets; ANOVA, $P < 0.001$. *Different from all, $P < 0.04$. *B*: *Gcg*/*Ppib* increased in STZ-saline islets and significantly reverted to control levels in STZ-IMT504 islets; ANOVA, $P < 0.001$. #Different from all, $P < 0.002$. *C*: *Sst*/*Ppib* increased in STZ-saline islets and significantly reverted to control levels in STZ-IMT504 islets; ANOVA, $P < 0.02$. *Different from all, $P < 0.03$. *D*: *Ins1*/*Ppib* did not vary among the experimental groups; ANOVA, NS. *E*: *Ppy*/*Ppib* did not vary among the experimental groups; ANOVA, NS. *F*: *Pdx1*/*Ppib* tended to decrease in STZ-saline and STZ-IMT504 islets but did not attain statistical significance; ANOVA, NS. *G*: *Mafa*/*Ppib* significantly decreased in STZ-saline and STZ-IMT504 islets with regard to control-saline; ANOVA, $P < 0.04$. *Different from STZ-saline and STZ-IMT504, $P < 0.03$. *H*: *Nes*/*Ppib* increased in STZ-saline islets and significantly reverted to control levels in STZ-IMT504 islets; ANOVA, $P < 0.01$. *Different from all, $P < 0.03$. *I*: *Reg1*/*Ppib* increased in STZ-saline islets compared with controls, whereas the expression partially reverted in STZ-IMT504 islets; ANOVA, $P < 0.02$. *Different controls, $P < 0.01$. *J*: *Cxcl1*/*Ppib* increased in STZ-saline islets and significantly reverted to control levels in STZ-IMT504 islets; ANOVA, $P < 0.05$. *Different from all, $P < 0.04$. *K*: *Pecam1*/*Ppib* increased in control-IMT504 and STZ-IMT504 islets, suggesting an IMT504-specific effect; ANOVA, $P < 0.01$. *Different from control-saline and STZ-saline, $P < 0.03$. *L*: *Reg2*/*Ppib* increased in STZ-IMT504 islets, suggesting the participation of this gene in the regeneration of β-cells induced by IMT504; ANOVA, $P < 0.02$. *Different from controls, $P < 0.05$.

ferentiation induced by STZ damage, as also demonstrated in other β-cell loss models (6, 44, 45).

Regarding gene regulation, a group of genes was upregulated by islet damage, and their expression was normalized by IMT504 at a time when diabetes control was already evident. Among them, *Ins2* increased its expression probably as a compensatory response to β-cell loss. *Gcg* and *Sst* have been shown to increase upon β-cell damage (45), in agreement with our results. *Nes* was induced by islet damage and reversed by IMT504. These results differ from our results in toxic diabetes

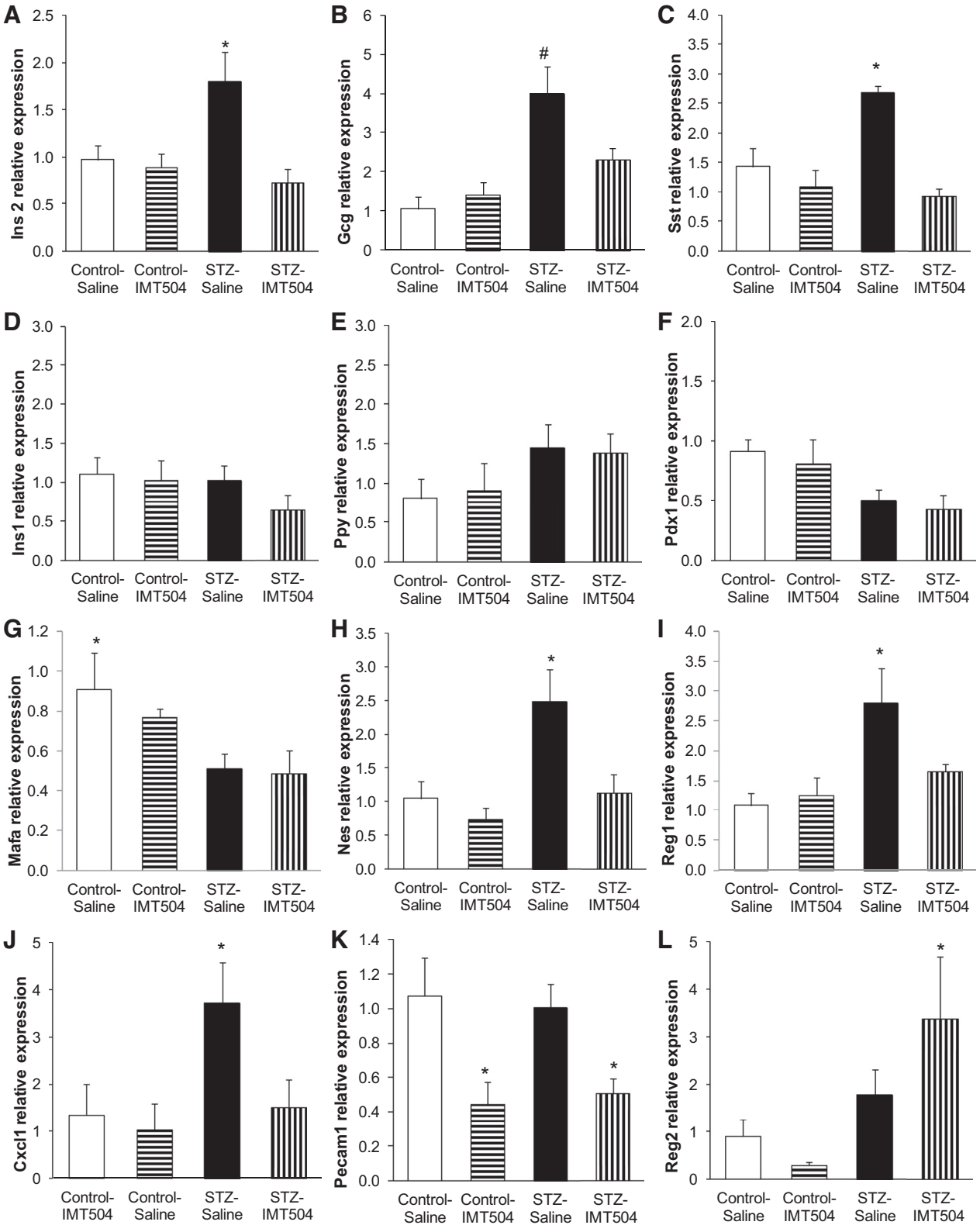

in rats, in which IMT504 stimulated nestin protein expression (3). Whether the difference is related to the species or the diabetes model is not clear. Nevertheless, in agreement with our present results, Tonne et al. (46) demonstrated increased *Nes* expression by immunological damage in another mouse diabetes model. We also evaluated members of the regeneration gene family (Reg), as several groups have identified members of this family as being expressed in T1D and during the process of whole islet neogenesis and β-cell regeneration in the pancreas (2, 20, 24, 32). *Reg1* showed a similar pattern of expression to *Ins2*. *Reg1* was shown to increase in T1D (32), and it was also related to β-cell death when overexpressed (36). In agreement with these descriptions, *Reg1* was increased in MLDS islets that showed an increased apoptotic index. In the cases of *Ins2*, *Gcg*, *Sst*, *Nes*, and *Reg1*, we interpret the decreases in expression after IMT504 treatment as a sign of islet recovery.

CXCL1 is expressed by macrophages, neutrophils, and epithelial cells and has neutrophil chemoattractant activity. Interestingly, increased plasma CXCL1 was observed in T1D patients (21). Moreover, during inflammation, pancreatic macrophages and β-cells produce this chemokine, recruiting leucocytes from blood to the islets (10). The reduced *Cxcl1* expression in IMT504-treated diabetic islets may reflect islet recovery or it may imply an IMT504-specific effect, since IL-6 (increased by IMT504) suppresses local CXCL1 expression, contributing to the control of inflammation (34), suggesting another possible mechanism of action for IMT504.

Other genes encoding for adult β-cell-specific transcription factors were downregulated by STZ-induced damage, such as *Pdx* and *Mafa*, and this inhibition was not reversed by IMT504, even though diabetes parameters had improved. Although *Pdx1* and *Mafa* have been shown to regulate *Ins2* expression, in our experimental conditions no correlation was observed. Since *Reg1* showed the same pattern as *Ins2*, we hypothesize that in these conditions *Reg1* may be driving *Ins2* expression.

Interestingly, some genes showed an IMT504-specific response. In the case of *Pecam1*, a significantly decreased expression was observed in both IMT504-treated control and diabetic islets, demonstrating an ODN-specific response. PECAM-1 is normally found on endothelial cells, macrophages, T/NK cells, and lymphocytes, among other cells. PECAM-1 plays a functional role mediating leukocyte migration through the perivascular basement membrane (8). Our results suggest that a decrease in *Pecam1* expression could inhibit leukocyte migration into islets, reducing infiltration, a very significant feature of IMT504-treated diabetic mice. *Reg2* showed a different pattern from *Reg1*; it tended to increase due to damage but was significantly upregulated by the combination of damage plus IMT504, indicating that it could be one of the mechanisms by which IMT504 induces β-cell regeneration, as evidenced by increased β-cell proliferation in the short-term analysis and recuperation of β-cell area in the long-term analysis. Similar to our results, other authors have demonstrated that Reg2 plays a dominant role in endogenous β-cell regeneration following adjuvant immunotherapy in diabetic mice (24, 25). Interestingly, all murine *Reg* genes carry one or more IL-6 response elements in their 5′ flanking region (20). Therefore, increased IL-6, as observed in STZ-IMT504 mice, could stimulate *Reg2* expression in islets, promoting β-cell restoration. Intriguingly, IL-6 is also expressed by β-cells (37), so a local increase in IL-6 could also contribute to the effects observed here.

Future work will analyze whether islet genes up- or downregulated by IMT504 are direct or indirect effects on islet cells, e.g., through circulating cytokines or other factors induced by this ODN. Moreover, translation of these gene products into proteins is necessary for them to exert the postulated effects, which will have to be corroborated.

In all, our results demonstrate that IMT504 induces significant improvement in blood glucose control, β-cell recovery, and clear inhibition of islet infiltration in immunodependent diabetic mice, and therefore, it may may be considered as a potential drug for T1D treatment. Furthermore, in preclinical toxicity studies, we demonstrated that IMT504 is a very safe drug (17, 23). We are presently validating the effects of IMT504 in NOD mice, a spontaneous model of T1D.

In conclusion, we propose that IMT504 meets the three criteria for a useful drug in autoimmune diabetes (18). *1*) It significantly maintains/restores β-cells, *2*) it markedly inhibits insulitis, and *3*) it is easy and cheap to synthesize and safe to administer. Considering these facts, further preclinical and clinical studies to assess the efficacy of the IMT504 in autoimmune diabetes are warranted, in addition to determining its precise mechanism of action.

ACKNOWLEDGMENTS

We thank Dr. Jorge Zorzopulos (Immunotech, Buenos Aires, Argentina) for critical review of the manuscript. The F109-D12 and F55A10 hybridomas developed by Madsen were obtained from the Developmental Studies Hybridoma Bank, which was created by the National Institute of Child Health and Human Development and maintained at The University of Iowa, Department of Biology, Iowa City, IA.

GRANTS

This work was supported by Consejo Nacional de Investigaciones Científicas y Técnicas (PIP 2010-363 to C. Libertun and PIP 2013-571 to VLL), Agencia Nacional de Promoción Científica y Técnica (PICT 2013-061 to C. Libertun and PICT 2012 N° 707 to V. A. Lux-Lantos), Universidad de Buenos Aires (20020130100006BA 2014-2017 to C. Libertun), and Fundación René Barón, Argentina.

DISCLOSURES

The authors declare that there are no conflicts of interest associated with this article.

AUTHOR CONTRIBUTIONS

M.S.B., S.B., A.H.-I., L.M.M., N.L., and A.D.M. performed experiments; M.S.B., S.B., A.H.-I., L.M.M., N.L., A.D.M., and V.A.L.-L. analyzed data; M.S.B., N.A.C., A.D.M., and V.A.L.-L. interpreted results of experiments; M.S.B. prepared figures; M.S.B., C.L., N.A.C., A.D.M., and V.A.L.-L. edited and revised manuscript; C.L., N.A.C., A.D.M., and V.A.L.-L. approved final version of manuscript; A.D.M. and V.A.L.-L. conception and design of research; V.A.L.-L. drafted manuscript.

REFERENCES

1. **Aathira R, Jain V.** Advances in management of type 1 diabetes mellitus. *World J Diabetes* 5: 689–696, 2014.
2. **Akiyama T, Takasawa S, Nata K, Kobayashi S, Abe M, Shervani NJ, Ikeda T, Nakagawa K, Unno M, Matsuno S, Okamoto H.** Activation of Reg gene, a gene for insulin-producing beta -cell regeneration: poly(ADP-ribose) polymerase binds Reg promoter and regulates the transcription by autopoly(ADP-ribosyl)ation. *Proc Natl Acad Sci USA* 98: 48–53, 2001.
3. **Bianchi MS, Hernando-Insua A, Chasseing NA, Rodriguez JM, Elias F, Lago N, Zorzopulos J, Libertun C, Montaner A, Lux-Lantos VA.** Oligodeoxynucleotide IMT504 induces a marked recovery of STZ-in-

duced diabetes in rats: correlation with an early increase in the expression of nestin and Ngn3 progenitor cell markers. *Diabetologia* 53: 1184–1189, 2010.

4. **Bonaventura MM, Catalano PN, Chamson-Reig A, Arany E, Hill D, Bettler B, Saravia F, Libertun C, Lux-Lantos VA.** GABAB receptors and glucose homeostasis: evaluation in GABAB receptor knockout mice. *Am J Physiol Endocrinol Metab* 294: E157–E167, 2008.
5. **Chahin A, Opal SM, Zorzopulos J, Jobes DV, Migdady Y, Yamamoto M, Parejo N, Palardy JE, Horn DL.** The novel immunotherapeutic oligodeoxynucleotide IMT504 protects neutropenic animals from fatal Pseudomonas aeruginosa bacteremia and sepsis. *Antimicrob Agents Chemother* 59: 1225–1229, 2015.
6. **Chung CH, Hao E, Piran R, Keinan E, Levine F.** Pancreatic beta-cell neogenesis by direct conversion from mature alpha-cells. *Stem Cells* 28: 1630–1638, 2010.
7. **Coronel MF, Hernando-Insua A, Rodriguez JM, Elias F, Chasseing NA, Montaner AD, Villar MJ.** Oligonucleotide IMT504 reduces neuropathic pain after peripheral nerve injury. *Neurosci Lett* 444: 69–73, 2008.
8. **Dangerfield J, Larbi KY, Huang MT, Dewar A, Nourshargh S.** PECAM-1 (CD31) homophilic interaction up-regulates alpha6beta1 on transmigrated neutrophils in vivo and plays a functional role in the ability of alpha6 integrins to mediate leukocyte migration through the perivascular basement membrane. *J Exp Med* 196: 1201–1211, 2002.
9. **Di Giorgio NP, Semaan SJ, Kim J, Lopez PV, Bettler B, Libertun C, Lux-Lantos VA, Kauffman AS.** Impaired GABAB receptor signaling dramatically up-regulates Kiss1 expression selectively in nonhypothalamic brain regions of adult but not prepubertal mice. *Endocrinology* 155: 1033–1044, 2014.
10. **Diana J, Lehuen A.** Macrophages and beta-cells are responsible for CXCR2-mediated neutrophil infiltration of the pancreas during autoimmune diabetes. *EMBO Mol Med* 6: 1090–1104, 2014.
11. **Dienz O, Rincon M.** The effects of IL-6 on CD4 T cell responses. *Clin Immunol* 130: 27–33, 2009.
12. **Eleazu CO, Eleazu KC, Chukwuma S, Essien UN.** Review of the mechanism of cell death resulting from streptozotocin challenge in experimental animals, its practical use and potential risk to humans. *J Diabetes Metab Disord* 12: 60, 2013.
13. **Elias F, Flo J, Lopez RA, Zorzopulos J, Montaner A, Rodriguez JM.** Strong cytosine-guanosine-independent immunostimulation in humans and other primates by synthetic oligodeoxynucleotides with PyNTTTTGT motifs. *J Immunol* 171: 3697–3704, 2003.
14. **Fallarino F, Volpi C, Zelante T, Vacca C, Calvitti M, Fioretti MC, Puccetti P, Romani L, Grohmann U.** IDO mediates TLR9-driven protection from experimental autoimmune diabetes. *J Immunol* 183: 6303–6312, 2009.
15. **Fernández Vallone VB, Romaniuk MA, Choi H, Labovsky V, Otaegui J, Chasseing NA.** Mesenchymal stem cells and their use in therapy: what has been achieved? *Differentiation* 85: 1–10, 2013.
16. **Fontes JA, Rose NR, Cihakova D.** The varying faces of IL-6: From cardiac protection to cardiac failure. *Cytokine* 74: 62–68, 2015.
17. **Franco R, Rodriguez JM, Elias F, Hernando-Insua A, Flo J, Lopez R, Nagle C, Lago N, Zorzopulos J, Horn DL, Montaner AD.** Non-clinical safety studies of IMT504, a unique non-CpG oligonucleotide. *Nucleic Acid Ther* 24: 267–282, 2014.
18. **Giannoukakis N, Phillips B, Trucco M.** Toward a cure for type 1 diabetes mellitus: diabetes-suppressive dendritic cells and beyond. *Pediatr Diabetes* 9: 4–13, 2008.
19. **Gomez-Tourino I, Arif S, Eichmann M, Peakman M.** T cells in type 1 diabetes: Instructors, regulators and effectors: A comprehensive review. *J Autoimmun* 66: 7–16, 2016.
20. **Gurr W, Yavari R, Wen L, Shaw M, Mora C, Christa L, Sherwin RS.** A Reg family protein is overexpressed in islets from a patient with new-onset type 1 diabetes and acts as T-cell autoantigen in NOD mice. *Diabetes* 51: 339–346, 2002.
21. **Hakimizadeh E, Shamsizadeh A, Nazari M, Arababadi MK, Rezaeian M, Vazirinejad R, Jamali Z, Poor NM, Khorramdelazad H, Darakhshan S, Hassanshahi G.** Increased circulating levels of CXC chemokines is correlated with duration and complications of the disease in type-1 diabetes: a study on Iranian diabetic patients. *Clin Lab* 59: 531–537, 2013.
22. **Hernando IA, Montaner AD, Rodriguez JM, Elias F, Flo J, Lopez RA, Zorzopulos J, Hofer EL, Chasseing NA.** IMT504, the prototype of the immunostimulatory oligonucleotides of the PyNTTTTGT class, increases the number of progenitors of mesenchymal stem cells both in vitro and in vivo: potential use in tissue repair therapy. *Stem Cells* 25: 1047–1054, 2007.
23. **Hernando-Insua A, Rodriguez JM, Elias F, Flo J, Lopez R, Franco R, Lago N, Zorzopulos J, Montaner AD.** A high dose of IMT504, the PyNTTTTGT prototype immunostimulatory oligonucleotide, does not alter embryonic development in rats. *Oligonucleotides* 20: 33–36, 2010.
24. **Hill T, Krougly O, Nikoopour E, Bellemore S, Lee-Chan E, Fouser LA, Hill DJ, Singh B.** The involvement of interleukin-22 in the expression of pancreatic beta cell regenerative Reg genes. *Cell Regen (Lond)* 2: 2, 2013.
25. **Huszarik K, Wright B, Keller C, Nikoopour E, Krougly O, Lee-Chan E, Qin HY, Cameron MJ, Gurr WK, Hill DJ, Sherwin RS, Kelvin DJ, Singh B.** Adjuvant immunotherapy increases beta cell regenerative factor Reg2 in the pancreas of diabetic mice. *J Immunol* 185: 5120–5129, 2010.
26. **Kim N, Cho SG.** New strategies for overcoming limitations of mesenchymal stem cell-based immune modulation. *Int J Stem Cells* 8: 54–68, 2015.
27. **Klinker MW, Wei CH.** Mesenchymal stem cells in the treatment of inflammatory and autoimmune diseases in experimental animal models. *World J Stem Cells* 7: 556–567, 2015.
28. **Kota DJ, Wiggins LL, Yoon N, Lee RH.** TSG-6 produced by hMSCs delays the onset of autoimmune diabetes by suppressing Th1 development and enhancing tolerogenicity. *Diabetes* 62: 2048–2058, 2013.
29. **Krug A, Rothenfusser S, Hornung V, Jahrsdörfer B, Blackwell S, Ballas ZK, Endres S, Krieg AM, Hartmann G.** Identification of CpG oligonucleotide sequences with high induction of IFN-alpha/beta in plasmacytoid dendritic cells. *Eur J Immunol* 31: 2154–2163, 2001.
30. **Lee IF, van den Elzen P, Tan R, Priatel JJ.** NKT cells are required for complete Freund's adjuvant-mediated protection from autoimmune diabetes. *J Immunol* 187: 2898–2904, 2011.
31. **Lo B, Swafford AD, Shafer-Weaver KA, Jerome LF, Rakhlin L, Mathern DR, Callahan CA, Jiang P, Davison LJ, Stevens HE, Lucas CL, White J, von Borstel R, Todd JA, Lenardo MJ.** Antibodies against insulin measured by electrochemiluminescence predicts insulitis severity and disease onset in non-obese diabetic mice and can distinguish human type 1 diabetes status. *J Transl Med* 9: 203, 2011.
32. **Lu Y, Ponton A, Okamoto H, Takasawa S, Herrera PL, Liu JL.** Activation of the Reg family genes by pancreatic-specific IGF-I gene deficiency and after streptozotocin-induced diabetes in mouse pancreas. *Am J Physiol Endocrinol Metab* 291: E50–E58, 2006.
33. **Mauer J, Chaurasia B, Goldau J, Vogt MC, Ruud J, Nguyen KD, Theurich S, Hausen AC, Schmitz J, Bronneke HS, Estevez E, Allen TL, Mesaros A, Partridge L, Febbraio MA, Chawla A, Wunderlich FT, Bruning JC.** Signaling by IL-6 promotes alternative activation of macrophages to limit endotoxemia and obesity-associated resistance to insulin. *Nat Immunol* 15: 423–430, 2014.
34. **McLoughlin RM, Hurst SM, Nowell MA, Harris DA, Horiuchi S, Morgan LW, Wilkinson TS, Yamamoto N, Topley N, Jones SA.** Differential regulation of neutrophil-activating chemokines by IL-6 and its soluble receptor isoforms. *J Immunol* 172: 5676–5683, 2004.
35. **Mellor AL, Munn DH.** IDO expression by dendritic cells: tolerance and tryptophan catabolism. *Nat Rev Immunol* 4: 762–774, 2004.
36. **Nakagawa K, Takasawa S, Nata K, Yamauchi A, Itaya-Hironaka A, Ota H, Yoshimoto K, Sakuramoto-Tsuchida S, Miyaoka T, Takeda M, Unno M, Okamoto H.** Prevention of Reg I-induced beta-cell apoptosis by IL-6/dexamethasone through activation of HGF gene regulation. *Biochim Biophys Acta* 1833: 2988–2995, 2013.
37. **Ota H, Itaya-Hironaka A, Yamauchi A, Sakuramoto-Tsuchida S, Miyaoka T, Fujimura T, Tsujinaka H, Yoshimoto K, Nakagawara K, Tamaki S, Takasawa S, Kimura H.** Pancreatic beta cell proliferation by intermittent hypoxia via up-regulation of Reg family genes and HGF gene. *Life Sci* 93: 664–672, 2013.
38. **Paula FM, Leite NC, Vanzela EC, Kurauti MA, Freitas-Dias R, Carneiro EM, Boschero AC, Zoppi CC.** Exercise increases pancreatic beta-cell viability in a model of type 1 diabetes through IL-6 signaling. *FASEB J* 29: 1805–1816, 2015.
39. **Probert L.** TNF and its receptors in the CNS: The essential, the desirable and the deleterious effects. *Neuroscience* 302: 2–22, 2015.
40. **Radeff-Huang J, Seasholtz TM, Chang JW, Smith JM, Walsh CT, Brown JH.** Tumor necrosis factor-alpha-stimulated cell proliferation is mediated through sphingosine kinase-dependent Akt activation and cyclin D expression. *J Biol Chem* 282: 863–870, 2007.

41. **Rodriguez JM, Elias F, Flo J, Lopez RA, Zorzopulos J, Montaner AD.** Immunostimulatory PyNTTTTGT oligodeoxynucleotides: structural properties and refinement of the active motif. *Oligonucleotides* 16: 275–285, 2006.
42. **Rodriguez JM, Marchicio J, Lopez M, Ziblat A, Elias F, Flo J, Lopez RA, Horn D, Zorzopulos J, Montaner AD.** PyNTTTTGT and CpG immunostimulatory oligonucleotides: effect on granulocyte/monocyte colony-stimulating factor (GM-CSF) secretion by human CD56+ (NK and NKT) cells. *PLoS One* 10: e0117484, 2015.
43. **Skyler JS.** The year in immune intervention for type 1 diabetes. *Diabetes Technol Ther* 15, *Suppl* 1: S88–S95, 2013.
44. **Stanojevic V, Habener JF.** Evolving function and potential of pancreatic alpha cells. *Best Pract Res Clin Endocrinol Metab* 29: 859–871, 2015.
45. **Thorel F, Nepote V, Avril I, Kohno K, Desgraz R, Chera S, Herrera PL.** Conversion of adult pancreatic alpha-cells to beta-cells after extreme beta-cell loss. *Nature* 464: 1149–1154, 2010.
46. **Tonne JM, Sakuma T, Munoz-Gomez M, El Khatib M, Barry MA, Kudva YC, Ikeda Y.** Beta cell regeneration after single-round immunological destruction in a mouse model. *Diabetologia* 58: 313–323, 2015.
47. **Uccelli A, Prockop DJ.** Why should mesenchymal stem cells (MSCs) cure autoimmune diseases? *Curr Opin Immunol* 22: 768–774, 2010.
48. **Wang Z, Gleichmann H.** GLUT2 in pancreatic islets: crucial target molecule in diabetes induced with multiple low doses of streptozotocin in mice. *Diabetes* 47: 50–56, 1998.